In summary, our work on He^+ is the first use of an ion for precision g_J-factor comparisons. It offers the most promising opportunity to test the Z dependence of the g_J-factor theory for a hydrogenlike system. Using our current apparatus, we hope to improve the precision of our value to a few parts in 10^8 so that we will be able to criticize the radiative correction term $(\alpha/4\pi)(Z\alpha)^2$ to about 10%.

This work was supported by the National Science Foundation under Grant No. PHY77-22567.

[1]F. G. Walther, W. D. Phillips, and D. Kleppner, Phys. Rev. Lett. 28, 1159 (1972).
[2]H. Grotch and R. A. Hegstrom, Phys. Rev. A 4, 59 (1971).
[3]W. Happer, Rev. Mod. Phys. 44, 169 (1972).
[4]G. M. Keiser, H. G. Robinson, and C. E. Johnson, Phys. Lett. 51A, 5 (1975).
[5]G. M. Keiser, H. G. Robinson, and C. E. Johnson, Phys. Rev. A 16, 822 (1977).
[6]M. Pinard and M. Leduc, J. Phys. (Paris) 35, 741 (1974).
[7]J. S. Tideman and H. G. Robinson, Phys. Rev. Lett. 39, 602 (1977).

Demonstration of Resistive Inhibition of Fast Electrons from Laser-Produced Plasmas in Low-Density Gold Targets

D. J. Bond, J. D. Hares, and J. D. Kilkenny
Blackett Laboratory, Imperial College, London, SW72BZ, England
(Received 25 January 1980)

A numerical model is used to show that the range of suprathermal electrons from laser-produced plasmas can be significantly reduced by the electric field needed to drive a return current of cold electrons. Direct experimental evidence of a reduction of preheat by at least a factor of 3 is presented for targets containing a low-density gold layer.

PACS numbers: 52.50.Jm, 52.65.+z

It is now well established that when high-intensity light is incident on solid targets, a considerable fraction of the laser energy is converted into suprathermal electrons with a temperature T_H much greater than that of the thermal plasma.[1-3] Some of the energy of these electrons heats the target to comparatively large depths. Experiments with 1.06-μm lasers on layered targets containing K fluors[4] have measured the range of these suprathermal electrons and found that the range was consistent with the hard x-ray measurement of temperature and the Bethe-Bloch formula[5] for energy loss with scattering included. Preheat would have to be minimized for an ablative compression, and the use of a vacuum gap[6] might be one way of optimizing a *target* to prevent preheat. In this Letter we demonstrate an alternative target design for reducing the preheat range by including a high-resistivity, low-volume-density material within the target. The effect is explained simply; it is confirmed by a numerical simulation and by direct experimental measurements.

Consider a laser beam incident on a semi-infinite plane target. A fraction of the absorbed laser power is converted into suprathermal electrons flowing into the target carrying a current density j_H, which is typically 10^{10} A cm^{-2}.[4] The very-high-energy deposition rapidly ionizes the target which becomes a high-electron-density ($N_e \sim 10^{23}$ cm^{-3}), low-electron-temperature ($T_e \sim 200$ eV) plasma of resistivity η. Because such a plasma has a very small skin depth for the time scale of the laser pulse, a return current j_c must flow so that

$$j_H + j_c = 0.$$

The resistive electric field, $E = \eta j_c = -\eta j_H$, decelerates the suprathermal electrons, converting a part of their energy into Ohmic heating, ηj_c^2. If the collisional range of the suprathermal electrons is r_a (mass per area) and the target density is ρ then in the absence of electric field inhibition the suprathermal electrons will go a distance r_a/ρ, and the electrostatic potential a distance r_a/ρ into the target will be $\sim \eta j_H r_a/\rho$. However if $\eta j_H r_a/\rho \gtrsim kT_H/e$ the resistive electric field will appreciably impede the suprathermal electrons. The potential within the target is estimated in Table I for solid-density gold and for gold at 1% of its solid density (0.2 g cm^{-3}), with $j_H = 10^{10}$ A cm^{-2} for 100 ps as suggested by experi-

TABLE I. Estimates of the potential within the target for the density of solid gold and for 1% of that density.

Density	Target thickness X (μm)	Current density j_H (A cm^{-2})	Resistivity η (LTE and Spitzer) (Ω cm)	Potential $j_H \eta X$ (V)
Solid	0.5	10^{10}	8×10^{-5}	40
1% Solid	50	10^{10}	4×10^{-4}	2×10^{4}

ment.[4] The resistivity is calculated for local thermodynamic equilibrium (LTE)[7] and Spitzer resistivity.[8] It is clear that in normal gold, the target potential is negligible compared with the electron energy, whereas in low-density gold the target potential will be large and thus the suprathermal electrons will be inhibited by the resistive electric field. The three factors in low-density gold which enhance this inhibition are (i) the large stopping distance r_a/ρ at low density, (ii) the high state of ionization (~30) achieved for small temperature rise in gold, and (iii) the larger LTE state of ionization at lower electron density for a given T_e.

To predict the effect of the resistive electric field we have used a Monte Carlo calculation with a self-consistent electric field. Hydrodynamics and thermal and radiation transport are neglected. The transport of the fast electrons at any one time is solved iteratively by a time-independent Monte Carlo transport calculation in slab geometry. The scattering is represented by a random Rutherford scattering from Fermi-screened nuclei and Debye-shielded ions. In between the scattering events, electrons follow parabolic trajectories representing the effect of the resistive field. A new electric field is determined from Ohm's law with a resistivity given by the equation of state for the local energy deposition and Ohmic heating up to that time, and $j_c = -j_H$ is determined from the transport calculation. The electron transport is then iterated to find a consistent E and j_H. The collisional energy deposition is calculated with use of the continuous slowing-down approximation accounting for bound electrons[5] and plasma electrons.[9]

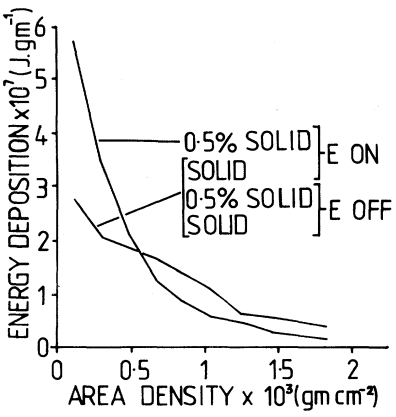

FIG. 1. Computational results for solid and low-density targets. At the rear of the low-density target ~50% of the deposition is due to $\vec{J}\cdot\vec{E}$ heating by the return current.

The calculation was used to simulate typical experimental parameters. Experiments at $I = 3\times10^{15}$ W cm^{-2} indicate that the fast-electron energy spectrum is of the form $f(u) = u^{3/2}\exp(-u/kT_H)$ with $T_H = 14$ keV, with 8% of the incident energy in this distribution. Figure 1 shows that in the solid-density gold targets the resistive field has a negligible effect, whereas for low-density gold the range is reduced because of the resistive electric field.

To confirm the effect, an experiment was performed with tracer layers to detect fast electrons by the $K\alpha$ radiation they produced.[4] Targets were normally irradiated with 20-J, 90-ps, 1.05-μm laser pulses focused with an $f/1$ lens to a 100-μm-diam spot, at an intensity of 2.8×10^{15} W cm^{-2}. The targets consisted of 1.5 μm Al, 3 μm KCl, gold, and 3 μm CaF_2, and were fabricated by evaporating the various layers onto the aluminum substrate. The gold layer was deposited at various densities. Solid gold layers were made by vacuum evaporation; low-density layers (~1% solid density) were made by slowly evaporating the gold in an atmosphere of 50 mbar of argon, thus creating voids in the gold. The targets were constructed in pairs of similar area mass density but with solid- and ~0.6% solid-density gold. The area density of the low-density targets was determined by weighing and measuring their depth with a scanning electron microscope. The struc-

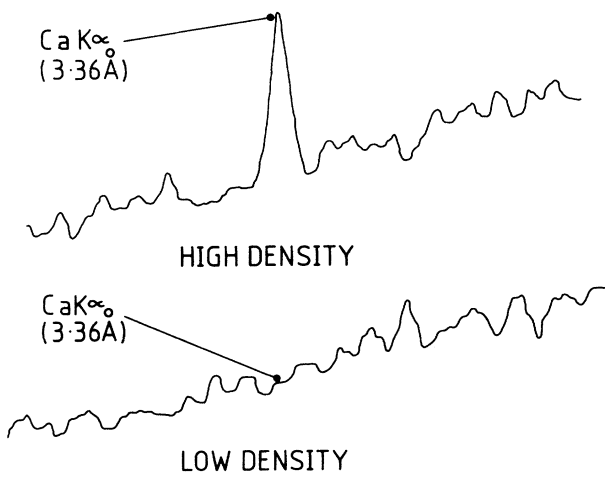

FIG. 2. Microdensitometer tracings in the region of the calcium $K\alpha$ line for a typical pair of targets with ~1 mg cm^{-2} of high- and low-density gold. The sensitivity is the same in both cases. The potassium $K\alpha$ yield measured by the front spectrometer was slightly higher for the low-density case.

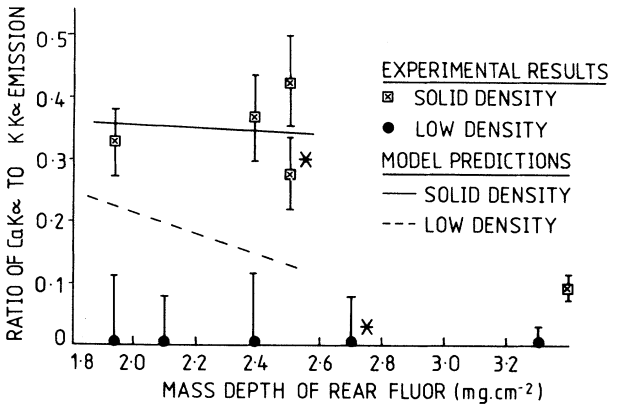

FIG. 3. Ratio of rear to front $K\alpha$ emission for pairs of targets with high- and low-density gold. The pair shown in Fig. 2 is represented by stars. The predicted inhibition is shown and is less than the observed inhibition.

ture of the low-density gold is of a submicron scale length. Expansion velocities are sufficiently high that it becomes uniform before the peak of the laser pulse.

The laser was incident on the aluminum which provided a flat and well-characterized ablation plasma. The Ca in CaF_2 and K in KCl acted as fast-electron detectors by the $K\alpha$ emission that was induced in them.[4] The gold acted as a variable-density electron filter. However, as shown below, the depth within the target of the gold reduced the resistive inhibition effects.

The $K\alpha$ emission was recorded by two miniature flat-crystal spectrometers. One spectrometer, at the front of the target, recorded the K $K\alpha$ emission and the Al plasma radiation. The other, at the rear, recorded the Ca $K\alpha$ emission.

A typical tracing of the Ca $K\alpha$ line for low- and high-density gold of the same area density is shown in Fig. 2. With low-density gold there is no observable $K\alpha$ line. The yields either side of the gold are shown in Fig. 3. For one shot 0.05 μm of KCl was deposited on the front of the target. From the attenuation of the heliumlike resonance lines, the area density of the gold was confirmed. It is clear that low-density gold reduces the $K\alpha$ yield, and therefore the energy deposition by fast electrons, by at least a factor of 3 over the same area density of high-density gold.

The $K\alpha$ yields predicted by the Monte Carlo calculation are also shown in Fig. 3. The inhibition predicted for low-density gold is small compared with the case in Fig. 1, because of the large amount of material that electrons have to pass through before they reach the gold. The predicted inhibition in Fig. 3 is also less than observed experimentally. This is probably due to defects in the model, the most noticeable being the application of the Spitzer formula to a low-$\ln\Lambda$ (~2) partially stripped plasma where the minimum impact parameter is less than or about the size of the atoms. The modeling was repeated with increased coefficients of resistivity. A factor-of-3 increase in resistivity brought the low-density Ca $K\alpha$ yields just inside the experimental error bars.

In conclusion we have shown both theoretically and experimentally that specific fast-electron energy deposition can be greatly increased by the use of a suitable low-density target material. This effect could be advantageous in ablative type compressions. For targets with high- and low-density layers of similar area mass density, a large irradiance may be used with the low-density target before preheat becomes important.

The experiment described in this Letter was performed at the Rutherford Laboratory Central Laser Facility.

[1]D. W. Forslund, J. M. Kindel, and R. Lee, Phys.

Rev. Lett. 39, 284 (1977).

[2]P. M. Campbell *et al.*, in *Proceedings of the Sixth International Conference on Plasma Physics and Controlled Nuclear Fusion Research, Berchtesgaden, West Germany, 1976* (International Atomic Energy Agency, Vienna, 1977), Vol. 1.

[3]E. K. Storm *et al.*, University of California Radiation Laboratory Report No. UCRL 50021-76, 1977 (unpublished), pp. 5.85–5.126.

[4]J. D. Hares, J. D. Kilkenny, M. H. Key, and J. G. Lunney, Phys. Rev. Lett. 42, 1216 (1979).

[5]H. A. Bethe, Ann. Phys. (Leipzig) 5, 325 (1930).

[6]K. Lee, D. W. Forslund, J. M. Kindel, and L. E. Lindman, Nucl. Fusion 19, 1447 (1979).

[7]Ya. B. Zel'dovich and Yu. P. Raizer, in *Physics of Shock Waves and High Temperature Hydrodynamic Phenomena*, edited by W. D. Hayes and R. F. Probstein (Academic, New York, 1967), p. 201.

[8]L. Spitzer and R. Harm, Phys. Rev. 89, 977 (1953).

[9]D. Pines and D. Bohm, Phys. Rev. 85, 338 (1952).